Contents lists available at ScienceDirect

Thin Solid Films

journal homepage: www.elsevier.com/locate/tsf

Optimizing cathodic electrodeposition parameters of ceria coating to enhance the oxidation resistance of a Cr_2O_3-forming alloy

Xu Wang *, Fan Fan, Jerzy A. Szpunar

Department of Mechanical Engineering, University of Saskatchewan, Saskatoon, SK, S7N 5A9, Canada

ABSTRACT

Nano-ceria coating was deposited onto a chromium oxide forming alloy through galvanostatic cathodic electro-deposition method in cerium nitrate electrolyte. The electrochemical behavior and influence of main deposition parameters of current density, deposition time, and temperature were studied. It was seen that the crystal size decreased with increasing of current density while micro-cracks were also observed at higher current density. Slightly increasing of crystal size and smoothing of surface morphology were seen with increasing of deposition time. It was reported that the bath temperature has the most significant effect on crystal size and surface morphology of the deposit. Green rust as corrosion product was also observed with deposition temperatures higher than 35 °C. Optimized deposition parameters were used to produce homogeneous, continuous and green rust-free coatings which enhance the oxidation resistance of alloy 230. The electro-deposition process was found to be an accessible and efficient method to prepare nano-crystalline ceria coating.

1. Introduction

Protective oxide layers are necessary for alloys which are expected to be used in high temperature environments. These protective layers, in general, are accepted as diffusion barriers which should be high temperature stable, densely compact and well adhesive to the substrates [1]. Therefore, alloys which are able to form chromium oxide (Cr_2O_3) or aluminum oxide (Al_2O_3) layers can be used for high temperature applications. These alloys are named as Cr_2O_3-forming and Al_2O_3-forming alloys.

Minor addition of rare earth elements like Ce, Hf, Dy and Yb can significantly improve the high temperature oxidation behavior of Cr_2O_3 and Al_2O_3 forming alloys. This improvement was primarily termed as rare element effect (REE) since it was patented by Pfeil [2]. Recently, it was reported that not only the rare earth elements but also some other elements also have the similar influences on Cr_2O_3 and Al_2O_3 forming alloys. These previous works were summarized in several reviews [3–6]. Then the rare earth effect was renamed as reactive element effect (REE). Hereafter, the reactive element was defined as any element that has higher oxygen affinity than the oxide layer forming element which refers to Cr or Al. The benefits of REEs were mainly summarized as the reduction of oxidation rate and the enhancement of the adhesion between the oxide layer and the substrate. The hypotheses explain of how such a minor addition of REs could so strikingly enhance the oxidation behavior of materials were reported, but the exact reasons why this enhancement takes place are still not clearly known as summarized in a recent review [6].

Numerous methods have been used to add reactive elements either by alloying [7–11] or surface modification [12–18] in several materials. For instance, surface modification techniques like dip coating [13,18,19], sputtering [20], ion implantation [21], electro-deposition [22,23], metal–organic chemical vapor deposition (MOCVD) [24], solution precursor plasma spray (SPPS) [25] were widely studied. Among these approaches, the electro-deposition was considered as one of the most promising, efficient and environmental friend ways to produce stable and homogeneous metal oxide thin films. It was reported that the chemical composition, surface morphology and thickness of the produced film could be controlled by changing the deposition parameters of electrical potential, current density and bath temperature [17,26–29]. However, until now, studies on the influence of ceria coatings produced by electrochemical deposition were mainly focusing on Al_2O_3-forming alloys [23, 29–35]. Research on the effect of electrochemical deposition of ceria on the oxidation behavior of Cr_2O_3-forming alloys was barely reported.

Therefore, the purpose of this work is to optimize the electro-deposition parameters such as the current density, deposition time and bath temperature to produce homogeneous ceria coatings which could be used to enhance the oxidation resistance of Cr_2O_3-forming alloys.

* Corresponding author.
  E-mail address: xuw388@mail.usask.ca (X. Wang).

2. Experimental procedure

2.1 Material

Nickel-based alloy Haynes 230 is used in present work with its nominal chemical composition shown in Table. 1. As a promising candidate structural material for the very high temperature reactor (VHTR), Haynes 230 is expected to be used at 900 to 1000 °C for at least 60 years. Therefore, many works have attempted to investigate the oxidation behavior of this alloy at different temperatures from 650 to 1150 °C [36–43]. However, methods for enhancing the oxidation behavior of this alloy were barely reported.

Specimens with dimensions of 30 mm × 20 mm × 1 mm were cut from the alloy sheet and mechanically polished up to 1200 grit SiC emery paper. Then all the specimens were ultrasonically cleaned in acetone for 10 min, washed with deionized water and ethanol and immediately dried under flowing air before deposition of ceria coating.

2.2 Preparation of ceria coating

Ceria coating was synthesized by cathodic electrochemical deposition (CED) method. The CED was completed using a classical three-electrodes Gamry Interface 1000 experimental device which includes the sample as working electrode, a Pt grid or graphite as a counter electrode and saturated calomel electrode (SCE) as a reference electrode. 0.1 M $Ce(NO_3)_3$ $6H_2O$ was used as an electrolyte solution. All the specimen surfaces were deposited with ceria. To find a proper counter electrode and appropriate electro-deposition parameters, the potentiodynamic measurements with a linear sweep rate of 1 mV/s were recorded both with Pt and graphite counter electrode. The low sweep rate will offer enough time for the reactions to follow the potential change and arrive at a quasi-stationary state. Before application of current, all the electrodes were kept in the electrolyte for 10 min to establish a quasi-stable open-circuit potential. The galvanostatic mode was used to operate the deposition processes with different current densities of −0.5, −0.75, −1, −1.5, −2 and −2.5 mA/cm^2 to investigate how current density affects the formation of the ceria films. Furthermore, the ceria films were produced with different deposition times from 2 to 20 min to study the influence of deposition time. Finally, various bath temperatures were used to prepare the reactive element coatings. After depositing, the samples were washed with ethanol, dried by hot dryer and then dried in a desiccator for 24 h before any characterization. Cleaning of the deposits by ethanol will release the nitrides and CO_2 incorporated in the deposited films [17,27,28].

2.3 Oxidation process

After optimizing the deposition parameters, we could obtain a very homogeneous and uniform coating on top of the specimen. Therefore, all the samples both with and without coating were oxidized at 900 °C in a muffle furnace to see if the coating could enhance the oxidation resistance of the substrate. All samples were weighed before and after oxidation by a METTLER TOLEDO XS205 dual range analytical balance with an accuracy of 0.01 mg.

2.4 Characterization technique

The phase identification of the deposited ceria film was characterized using D8 Bruker discovery X-ray diffraction (XRD) with a Cr Kα radiation and 2D Hi-star detector at a scanning rate of 1°/min and step size

of 0.01°. The voltage and current for XRD measurements were 40 kV and 40 mA. 2θ ranging from 20° to 100° was scanned for the sample. The surface morphology of deposit was characterized by Hitachi SU6600 scanning electron microscope (SEM) at 5 kV. Energy dispersive spectroscopy (EDS) system mounted on Hitachi SU6600 was used to determine the chemical components of the deposits at 15 kV. EDS was done at a resolution of 1024 × 1024 with a pixel dwell time of 300 μs.
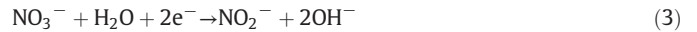
Renishaw 2000 Raman microscope with laser source wavelength of 785 nm was also used to characterize the deposits.
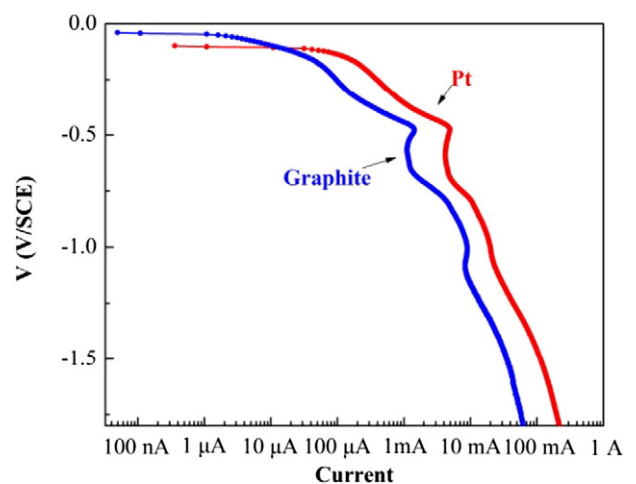
3. Results and discussions

3.1 Electrochemical characterization

Fig. 1 shows the cathodic potentiodynamic scanning curve of Haynes 230 with Pt and graphite counter electrode. As can be seen from this figure, the electro-deposition process with Pt counter electrode gains a higher current density than that with a graphite electrode. In other words, the deposition potential needed for Pt electrode is reduced for the same current density. Therefore, Pt grid is used as the counter electrode since it can obtain a higher cathodic current efficiency.

The mechanism of electro-deposition using nitrate baths has been investigated and discussed by other researchers [17,27]. Three continuous steps were suggested by Bouchaud [17] and Hamlaoui [27,28] for the potentiodynamic curve. During the lower potential stage, the potential variation may because of oxygen, nitrate reduction and the Reactions (1) to (3) may present. Reaction (1) may also happen through two step reactions as shown in Eqs. (4) and (5).

$$O_2 + 2H_2O + 4e^- \rightarrow 4OH^- \tag{1}$$

$$2H_2O + 2e^- \rightarrow H_2 + 2OH^- \tag{2}$$

$$NO_3^- + H_2O + 2e^- \rightarrow NO_2^- + 2OH^- \tag{3}$$

$$O_2 + H_2O + 2e^- \rightarrow HO_2^- + OH^- \tag{4}$$

$$HO_2^- + H_2O + 2e^- \rightarrow 3OH^-. \tag{5}$$

The second step corresponds to the potential drop which refers to the film deposition process. During this stage, a continuous and homogeneous deposit layer forms which may result from the Reactions (6) to (7). The OH^- produced from the first step allows the formation of $Ce(OH)_3$ or $Ce(OH)_2^{2+}$.

$$Ce^{3+} + 3OH^- \rightarrow Ce(OH)_3 \tag{6}$$

Fig. 1. Cathodic potentiodynamic scan of alloy 230 with Pt and graphite counter electrode.

Table 1
Nominal chemical composition of Haynes 230 (wt.%).

Ni	Cr	W	Mo	Fe	Co	Mn	Si	Al	C	La	B
Bal	22	14	2	3	5	0.5	0.4	0.3	0.1	0.02	0.01